Stable Isotope Geochemistry: A Tribute to Samuel Epstein
© The Geochemical Society, Special Publication No. 3, 1991
Editors: H. P. Taylor, Jr., J. R. O'Neil and I. R. Kaplan

$^{13}C/^{12}C$ ratios of the Fe(III) carbonate component in natural goethites

CRAYTON J. YAPP and HARALD POTHS
Department of Geology, University of New Mexico, Albuquerque, NM 87131, U.S.A.

Abstract—Small amounts of CO_2 are evolved during incremental vacuum dehydration of natural goethites at *ca.* 230°C. Much of the CO_2 appears to originate in a minor Fe(III) carbonate component in goethite. The amounts of the putative Fe(III) carbonate (also referred to as trapped CO_2) in the samples of this study range from 0.041 to 0.14 μmoles of CO_2 per milligram of goethite. The $\delta^{13}C$ values of this trapped CO_2 range from −17.1 to +2.9 per mil. While temperatures and pH may affect the $\delta^{13}C$ values of the Fe(III) carbonate component in goethites, differences in the $\delta^{13}C$ values of the ambient aqueous carbonate systems probably account for much of the observed $\delta^{13}C$ range of about 20 per mil.

INTRODUCTION

THE SOLID-STATE phase transformation of natural goethite to hematite in vacuum at temperatures of *ca.* 230°C is accompanied by the release of CO_2 (YAPP, 1983, 1987a; YAPP and POTHS, 1986). YAPP and POTHS (1986) used isotopic and material-balance results to demonstrate that this evolved CO_2 originated predominantly from two sources: (1) organic matter and (2) an inorganic CO_2-bearing component "trapped" within the goethite structure. Discrete admixed carbonate phases such as siderite, calcite, dolomite, etc. were experimentally ruled out as probable sources of the inorganically derived CO_2, because these minerals do not decarbonate at 200 to 300°C in vacuum on the time scales of the goethite dehydration experiments. YAPP and POTHS (1986) were able to calculate the $\delta^{13}C$ values of the organic matter associated with some of the goethites by measuring total carbon abundances and $\delta^{13}C$ values before and after treatment with concentrated hydrogen peroxide solution at room temperature. However, their experiments could not provide information on the $\delta^{13}C$ value of the CO_2 evolved from the inorganic source within the goethite.

YAPP (1987a) hypothesized that the inorganically derived CO_2 ("trapped" CO_2) might originate from an Fe(III) carbonate component in solid solution in goethite. YAPP and POTHS (1990) presented infrared spectral evidence for a distorted carbonate molecule in natural goethites. The wavenumbers of the carbonate absorption peaks were similar to those measured by DVORAK *et al.* (1969) for an unstable synthetic Fe(III) carbonate and support the idea of an Fe(III) carbonate component in the goethite crystal structure. The results of YAPP and POTHS (1986) and YAPP (1987a) indicate that, although unstable, the putative Fe(III) carbonate component in goethite will not decompose to release CO_2 unless the confining goethite structure also breaks down. This behavior implies that the Fe(III) carbonate ("trapped CO_2") which was incorporated in the goethite at the time of goethite formation will likely remain a closed system until the goethite structure is disrupted. Experiments to measure the concentrations and $\delta^{13}C$ values of trapped CO_2 in natural goethites and the paleoenvironmental implications of the results are considered in this paper.

EXPERIMENTAL METHODS

Samples of five natural goethites from diverse locales were selected for this study. The five were chosen because their total carbon $\delta^{13}C$ values before H_2O_2 treatment represent a relatively large range from −26.5 to −8.1 (see Table 1). The samples are labeled Paleo-X, OPWis-9, SConn-1, PPColo-1, and NMx-2. Paleo-X is a pseudomorph of goethite after pyrite from an occurrence in the Lucero Mountains of New Mexico. This sample was collected by S. Hayden. OPWis-9 is a sample of the Late Ordovician oolitic ironstone of the Neda Fm. collected by C. Yapp from the type locality in Wisconsin (PAULL, 1977). The remaining three goethite samples are described in YAPP and PEDLEY (1985). All five samples were ground to powders under reagent-grade acetone and sized by passage through brass sieves. Only the size fractions of less than 63 microns were employed in subsequent experiments (see YAPP and POTHS, 1986). Prior to grinding, the Neda Fm. sample (OPWis-9) was physically separated into ooliths and matrix. Only the ooliths from this deposit were used in this study. After grinding, all five samples were treated with 0.5 N HCl at room temperature for about 20 hours then thoroughly rinsed with deionized water. The dilute HCl treatment has no measurable effect on the goethite (YAPP, 1987b) and is employed to dissolve any calcite or aragonite that might be present in these samples as either an indigenous impurity or one introduced during handling. Any subsequent discussion of "untreated" samples refers to those powdered samples which have been subjected to only the dilute HCl rinse.

The results of YAPP and POTHS (1986) indicate that the removal of admixed organic matter will be necessary to facilitate straightforward determination of the $\delta^{13}C$ values of trapped CO_2 in goethites. These workers employed concentrated solutions of H_2O_2 (30%) to effect the removal of organic matter. For the present study the five afore-

Table 1. Total carbon yield and $\delta^{13}C$ values before and after H_2O_2 treatment. Trapped CO_2 yield before and after H_2O_2 treatment

	Total Carbon					Trapped CO_2 yield	
	Untreated		H_2O_2 treated				
Sample	Yield	$\delta^{13}C$	Yield	$\delta^{13}C$	W	Untreated	H_2O_2 treated
Paleo-X	0.13	−17.5	0.073	−10.0	0.44	0.045	0.041
OPWis-9	0.082	−19.8	0.052	−16.5	0.37	0.055	0.050
SConn-1	0.39*	−26.5*	0.081	−12.0	0.79	0.070*	0.055
PPColo-1	0.27*	−8.1*	0.19	+2.3	0.30	0.15*	0.14
NMx-2	0.45*	−19.5*	0.15	−3.1	0.67	0.13*	0.12

Yield reported as (μmoles C/mg sample).
W = fraction of total carbon removed by H_2O_2.
* Data from YAPP and POTHS (1986).

mentioned samples were subjected to room temperature treatments with concentrated H_2O_2 solutions for times ranging from 20 to 86 days using the approach of YAPP and POTHS (1986). In all cases the concentration of total carbon in the goethite was lower after H_2O_2 treatment, while the total carbon $\delta^{13}C$ value was more positive. Similar results were reported by YAPP and POTHS (1986) for three of these samples (SConn-1, PPColo-1, and NMx-2). All results on peroxide-treated samples reported in the current work were obtained on aliquots of these samples which were newly treated in quantities sufficient to permit incremental dehydration experiments.

The dehydration-decarbonation experiments were performed (after outgassing the sample at 100°C for one hour) under open system conditions in vacuum at temperatures ranging from 200 to 300°C. A sample was introduced into the furnace at a specified temperature for a predetermined amount of time. During this time the evolved CO_2 and H_2O were continuously recovered by freezing into a cold trap at liquid nitrogen temperatures. At the end of the specified time the mineral sample was removed from the furnace (while still under vacuum). The sample was kept in the room temperature portion of the evacuated dehydration chamber while the evolved CO_2 and water were separated and recovered for yield and isotopic measurements. After completion of the processing of this CO_2 and H_2O, the sample was reintroduced to the furnace (still under vacuum) for another specified time interval, and the evolved CO_2 and water were continuously collected in the liquid nitrogen-cooled cold trap. This procedure of incremental vacuum dehydration of an aliquot of goethite continued until there was little additional recovery of CO_2 or H_2O. Carbon and hydrogen which remained in the mineral after these incremental dehydration steps at "low" temperature were removed by dehydration at 850°C in about 0.16 bar of pure oxygen and recovered for measurement. Details of the dehydration-decarbonation vacuum system are given in YAPP (1983).

A small modification to the preceding procedure was introduced in experiments MHD-1087 and MHD-1090 (Tables 2 and 3). In these experiments the first dehydration step (after the outgassing at 100°C) was performed under closed-system conditions in 0.16 bar of pure O_2. YAPP (1983) observed that these kinds of closed-system conditions retarded the goethite dehydration. Consequently, it was felt that this low temperature combustion in the first dehydration step might result in removal of additional organic matter (perhaps remaining after the H_2O_2 treatment) without causing significant breakdown of the goethite.

Yields of incrementally evolved CO_2 were measured manometrically. The carbon isotope ratios of the CO_2 were measured on a Finnigan MAT Delta E isotope ratio mass spectrometer and are reported in the usual δ notation:

$$\delta^{13}C = \left[\frac{R(\text{sample})}{R(\text{standard})} - 1\right] \times 1000$$

where $R = {}^{13}C/{}^{12}C$ and the standard is PDB (CRAIG, 1957). The evolved water was quantitatively converted to hydrogen gas over uranium metal at 750°C and the hydrogen yield was measured manometrically. CO_2 yields were measured with a precision of about ±0.15 μmoles, while hydrogen yields were measured with a precision of about ±1 μmole. For CO_2 samples on the order of 1 μmole, the analytical error of $\delta^{13}C$ measurements is about ±0.3 per mil.

RESULTS AND DISCUSSION

The Fe(III) carbonate model for evolved CO_2

The results of the various dehydration-decarbonation experiments performed for this study are listed in Tables 2 and 3. With the exception of the untreated Paleo-X sample in Table 2, all the experiments of Tables 2 and 3 were performed as incremental dehydrations on a single aliquot of the sample in question. For the untreated Paleo-X material, each experiment involved only a single 230°C step followed by the 850°C combustion. Experiments of this type were run on four different aliquots of untreated Paleo-X to obtain information on the patterns of CO_2 and H_2O release and the $\delta^{13}C$ values of the evolved CO_2. Untreated Paleo-X was analyzed in this fashion, because at the time these experiments were run we were unable to accommodate the larger sample sizes required to perform incremental vacuum dehydrations on a single aliquot.

Table 2. Results from incremental dehydration-decarbonation experiments on natural goethites

MHD#	Time (min)	T (°C)	CO_2 μmoles	CO_2 $\delta^{13}C$	H_2 μmoles
	OPWis-9 (oolites) untreated				
1067	15	230	1.25	−13.0	150
1067	60	230	1.5	−16.1	260
1067	60	240	3.5	−17.6	322
1067	60	250	7.5	−17.4	649
1067	60	250	1.75	−17.4	193
1067	60	260	1.0	−19.2	122
1067	30*	850*	11.75	−23.5	188
	sample mass (after 100°C) = 344 mg				
	OPWis-9 (oolites) H_2O_2-treated				
1059	15	230	1.25	−12.4	82
1059	60	230	0.25	—	76
1059	60	240	1.5	−16.7	189
1059	60	250	2.0	−16.9	193
1059	60	250	1.35	−16.9	143
1059	60	250	1.0	−16.4	102
1059	30*	850*	2.0	−18.8	203
	sample mass (after 100°C) = 179 mg				
	OPWis-9 (oolites) H_2O_2-treated				
1090	60*	230*	1.6	−15.7	81
1090	30	230	0.9	−17.0	159
1090	30	230	1.25	−17.7	123
1090	45	230	2.8	−17.6	246
1090	60	230	2.8	−17.4	246
1090	60	230	1.25	−16.9	123
1090	120	230	0.3	—	41
1090	1080	230	~0.15	—	13
1090	30*	850*	1.25	−18.9	114
	sample mass (after 100°C) = 213 mg				
	Paleo-X untreated				
934	20	230	1.25	−6.8	139
934	30*	850*	11.75	−18.4	390
935	30	230	1.25	−7.0	139
935	30*	850*	9.75	−19.2	286
936	60	230	1.5	−6.5	193
936	30*	850*	9.0	−19.5	262
937	180	230	2.8	−7.2	408
937	30*	850*	9.75	−20.3	123
	Paleo-X H_2O_2-treated				
1073	15	230	2.0	−6.2	201
1073	60	230	4.5	−5.3	595
1073	60	230	2.0	—	319
1073	60	230	0.75	−5.3	139
1073	60	230	0.75	−6.5	129
1073	60	230	0.5	−6.5	55
1073	30*	850*	9.5	−14.8	330
	sample mass (after 100°C) = 326 mg				
	SConn-1 H_2O_2-treated				
1075	10	220	2.25	−11.1	307
1075	30	220	2.5	−11.1	319
1075	30	220	2.35	−10.5	260
1075	30	220	1.65	−11.3	171
1075	60	220	1.5	−12.3	163
1075	60	220	1.25	−14.3	96
1075	960	220	3.25	−21.5	114
1075	30*	850*	5.5	−14.5	102
	sample mass (after 100°C) = 250 mg				
	PPColo-1 H_2O_2-treated				
1060	45	200	4.25	−2.5	384
1060	60	200	2.25	+1.4	199
1060	60	200	2.75	+2.6	162
1060	60	200	1.75	+2.6	96
1060	60	200	2.75	+2.9	120
1060	60	200	2.0	+3.0	85
1060	90	200	2.5	+3.2	85
1060	180	200	2.75	+3.0	86
1060	3900	200	12.5	+3.4	368
1060	60	270	2.0	+1.1	42
1060	60	300	0.75	+2.6	19
1060	30*	850*	19.0	+2.8	115
	sample mass (after 100°C) = 281 mg				

* Indicates closed-system dehydration in about 0.16 bar of pure O_2.

Samples reported in YAPP and POTHS (1986) were also analyzed in the manner just discussed for untreated Paleo-X.

The model for an Fe(III) carbonate component in solid solution in goethite leads to some testable predictions under the following set of assumptions: (1) at temperatures of *ca.* 230°C the Fe(III) carbonate will break down to release CO_2 only when the local confining goethite structure breaks down; (2) the loss of structural hydrogen can be taken as a measure of the fraction of the goethite structure which has broken down to hematite; (3) the concentration of the Fe(III) carbonate component (trapped CO_2) is uniform throughout the goethite sample of interest; (4) the $\delta^{13}C$ value of the Fe(III) carbonate is uniform throughout the goethite sample of interest. If the trapped CO_2 is lost from lattice "compartments" during the thermal breakdown of goethite to hematite as suggested above, then in combination with the other assumptions it is ex-

Table 3. Dehydration-decarbonation experiments on NMx-2 goethite

MHD#	Time (min)	T (°C)	CO_2 μmoles	CO_2 $\delta^{13}C$	H_2 μmoles
1082	15	200	0.9	−8.5	123
1082	60	200	4.9	−2.7	414
1082	60	200	6.7	−0.5	320
1082	60	200	2.0	−0.1	71
1082	120	200	3.5	0.0	114
1082	120	200	0.8	−0.9	24
1082	1080	200	0.8	−8.1	28
1082	30*	850*	11.4	−5.5	100
	sample mass after (100°C) = 197 mg				
	NMx-2 H_2O_2-treated				
1087	60*	200*	3.2	−13.6	182
1087	15	200	0.0	—	58
1087	60	200	3.75	−0.9	396
1087	60	200	1.9	−0.2	106
1087	120	200	6.7	0.0	314
1087	120	200	5.4	0.0	216
1087	120	200	1.1	−0.3	45
1087	240	200	1.1	−0.3	41
1087	1200	200	1.6	−7.5	51
1087	30*	850*	14.9	−3.6	131
	sample mass (after 100°C) = 256 mg				

* Indicates closed-system dehydration in about 0.16 bar of pure O_2.

pected that the CO_2 and H_2O would be evolved in constant proportions. Thus,

$$\frac{n(CO_2)}{n(H_2O)} = m \qquad (1)$$

where

$n(CO_2)$ = μmoles of CO_2 evolved over an increment of vacuum dehydration-decarbonation,

$n(H_2O)$ = μmoles of H_2O evolved over that same increment, and

m = constant.

Equation (1) implies the following linear relation during dehydration-decarbonation of goethite:

$$X_s(CO_2) = [1 - X_s(CO_2)^*]X_s(H_2) + X_s(CO_2)^* \qquad (2)$$

where

$X_s(CO_2)$ = mole fraction of the initial total carbon that remains in the mineral after some interval of dehydration-decarbonation,

$X_s(H_2)$ = mole fraction of the initial total hydrogen that remains in the mineral after that same interval, and

$X_s(CO_2)^*$ = value of $X_s(CO_2)$ when $X_s(H_2) = 0$.

Also, because the model assumes that the Fe(III) carbonate is locally confined within the goethite lattice and breaks down only when the local lattice breaks down, the carbonate molecules should be incapable of exchanging carbon isotopes with one another or of being selectively removed because of different decomposition rates of the carbonate isotopic molecules. Thus, the $\delta^{13}C$ values of increments of "trapped" CO_2 evolved at *ca.* 230°C should be constant during the transformation of goethite to hematite. Figure 1 depicts representative predicted patterns of (a) evolved incremental CO_2 $\delta^{13}C$ values *vs.* $X_v(CO_2)$ and (b) $X_s(CO_2)$ *vs.* $X_s(H_2)$. $X_v(CO_2)$ is the cumulative sum of evolved CO_2 as a mole fraction of the total initial carbon in the sample. As shown in Fig. 1b and Eqn. (2), the slope and intercept of the linear $X_s(CO_2)$ *vs.* $X_s(H_2)$ curves depend

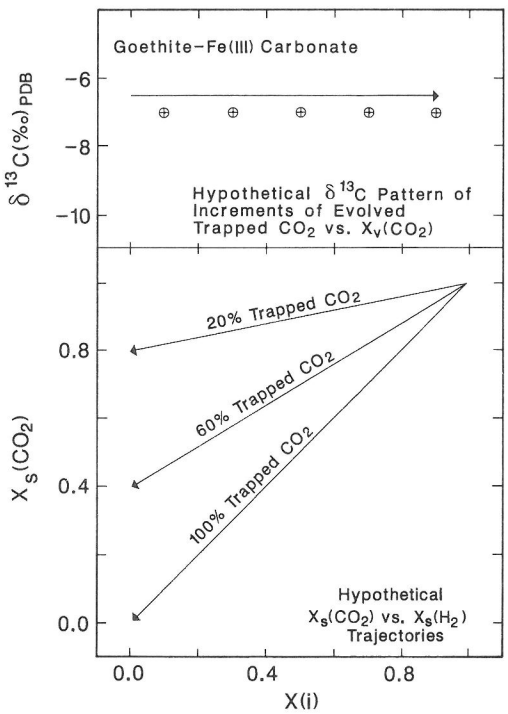

FIG. 1. Diagram at the top illustrates the constant $\delta^{13}C$ values expected for increments of CO_2 evolved from the Fe(III) carbonate component (trapped CO_2) in goethites as a function of fraction of total carbon removed [$X_v(CO_2)$]. The bottom graph depicts the pattern of $X_s(CO_2)$ *vs.* $X_s(H_2)$ expected during vacuum dehydration-decarbonation of H_2O_2-treated goethite. The percentage of the total carbon represented by trapped CO_2 (Fe(III) carbonate) determines the slope and intercept of the $X_s(CO_2)$ *vs.* $X_s(H_2)$ array. $X_s(H_2)$ is the fraction of total goethite hydrogen remaining in the mineral after some interval of dehydration. $X_s(CO_2)$ is the corresponding fraction of total carbon remaining in the mineral. See text for discussion of the model upon which these curves are based.

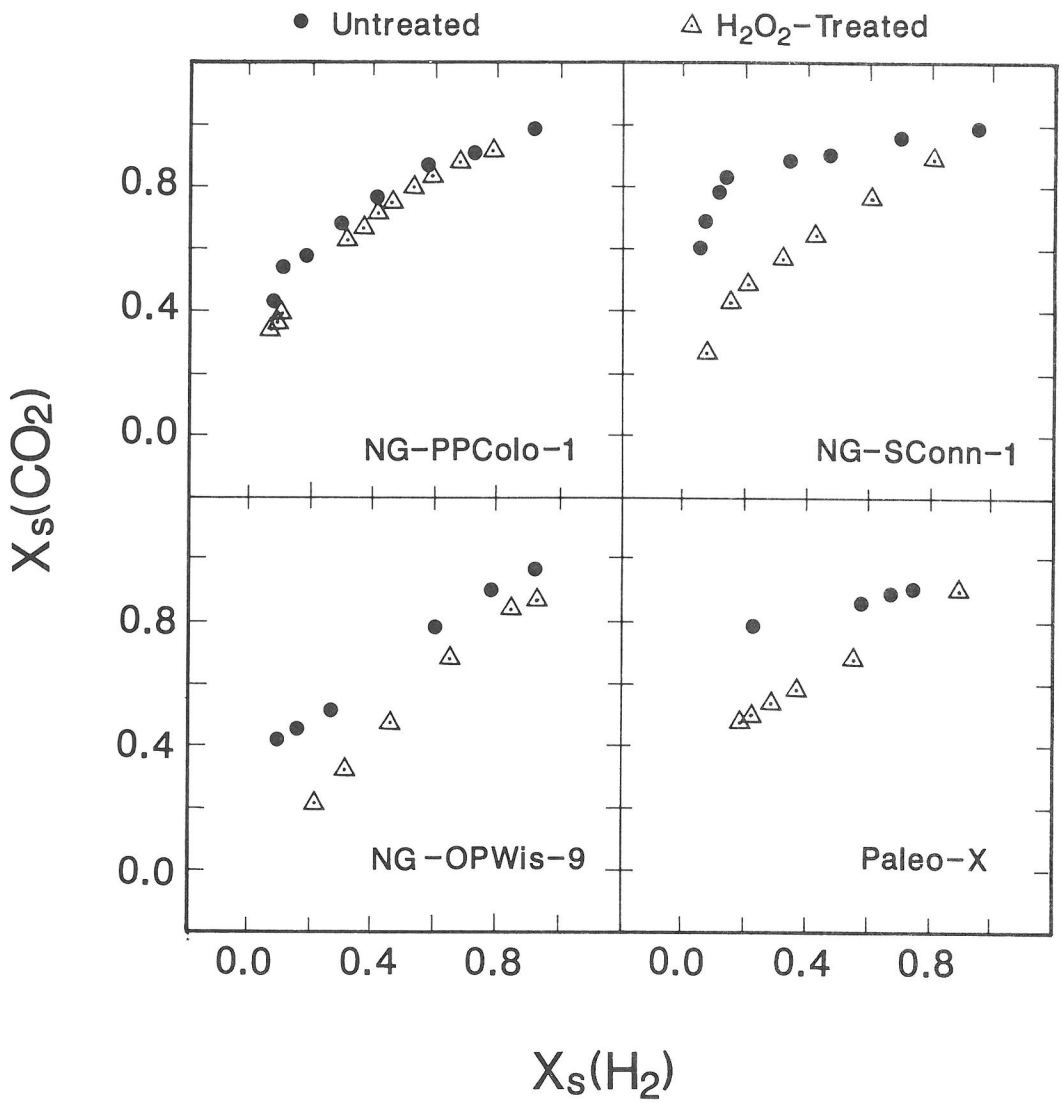

FIG. 2. $X_s(CO_2)$ *vs.* $X_s(H_2)$ for both untreated and H_2O_2-treated natural goethites. By comparison with Fig. 1 it is evident that the percentage of total carbon represented by trapped CO_2 (Fe(III) carbonate) is higher for an H_2O_2-treated sample aliquot than for a corresponding untreated aliquot. This is a consequence of removal of organic carbon in the H_2O_2-treated aliquots. The abrupt change in slope for the untreated SConn-1 data is discussed in the text.

upon how much refractory carbon $[X_s(CO_2)]^*$ is present in the goethite (*e.g.*, as admixed discrete carbonate phases). The amount of trapped CO_2 in a goethite sample as a mole fraction of the total carbon in the sample could be obtained by extrapolating a linear array of $X_s(CO_2)$ *vs.* $X_s(H_2)$ data points to the condition of complete removal of hydrogen. The mole fraction of trapped CO_2 would be equal to $[1 - X_s(CO_2)^*]$, which is also the slope of the line (Eqn. 2).

Plots of $X_s(CO_2)$ *vs.* $X_s(H_2)$ as calculated from the data of Tables 2 and 3 are shown in Figs. 2 and 3. The data for the untreated samples PPColo-1, SConn-1, and NMx-2 in Figs. 2 and 3 were taken from YAPP and POTHS (1986). It is evident from the data arrays in Figs. 2 and 3 that the removal of organic matter by treatment of the goethite samples with concentrated H_2O_2 solution has a significant effect on the patterns of release of CO_2 and H_2O. The effects are most pronounced in samples for which the initial amount of total carbon was high and removal of organic carbon by H_2O_2 was most extensive (SConn-1, 79% of carbon removed; and NMx-2, 67% removed, see Table 1). In the cases of

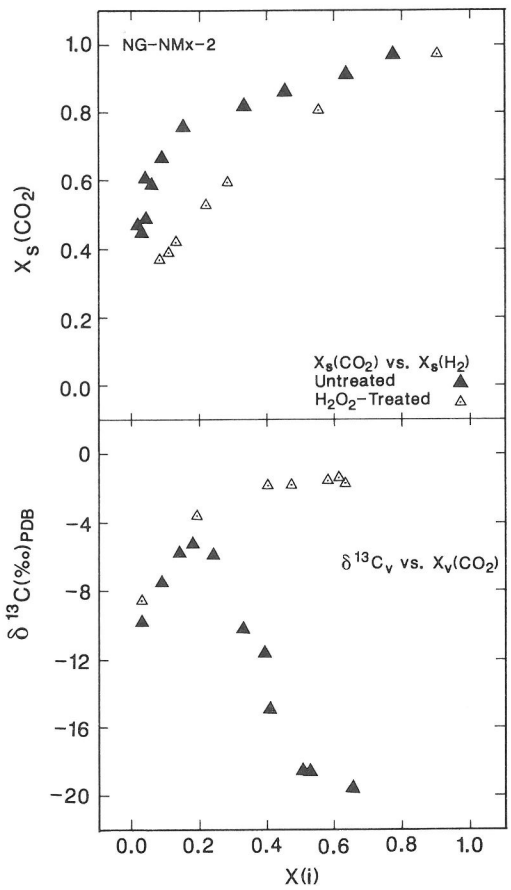

FIG. 3. Upper plot depicts $X_s(CO_2)$ *vs.* $X_s(H_2)$ for untreated and H_2O_2-treated NMx-2. The lower plot shows the variation of $\delta^{13}C_v$ with $X_v(CO_2)$. $\delta^{13}C_v$ is the $\delta^{13}C$ of the cumulative sum of CO_2 evolved at different extents of vacuum dehydration-decarbonation of goethite. $X_v(CO_2)$ is the cumulative sum of evolved CO_2 as a mole fraction of the total carbon in goethite. The contrasting patterns of $\delta^{13}C_v$ values for untreated and H_2O_2-treated NMx-2 reflect the increasing contribution of ^{13}C-depleted CO_2 slowly evolved from organic matter in the latter stages of the untreated goethite dehydration (see text for discussion).

untreated SConn-1 (Fig. 2) and untreated NMx-2 (Fig. 3) the plots of $X_s(CO_2)$ *vs.* $X_s(H_2)$ exhibit abrupt changes in slope at $X_s(H_2)$ values of about 0.18. As open-system goethite dehydration-decarbonation in vacuum at *ca.* 230°C progresses to $X_s(H_2)$ values less than about 0.20, the rate of further goethite breakdown decreases rapidly (YAPP, 1983). Experiments must be run for much longer times to achieve any further significant recovery of CO_2 and H_2O. As discussed by YAPP and POTHS (1986), the steeper slope of $X_s(CO_2)$ *vs.* $X_s(H_2)$ data arrays when $X_s(H_2)$ values are less than about 0.20 implies that a second source of carbon has begun to dominate the evolved CO_2 as trapped CO_2 becomes less important with the reduction in the rate of breakdown of goethite. YAPP and POTHS (1986) concluded that the second source of this slowly evolved CO_2 was organic matter. Because this organic-derived CO_2 is so slowly evolved, it should not be a major component of the CO_2 evolved early in the dehydration when the breakdown of goethite is rapid and the trapped CO_2 constitutes most of the recovered CO_2. Removal of most of the organic matter prior to dehydration-decarbonation of goethite should eliminate much of the abrupt change of slope in the $X_s(CO_2)$ *vs.* $X_s(H_2)$ arrays of untreated SConn-1 and NMx-2 in Figs. 2 and 3. The patterns of $X_s(CO_2)$ *vs.* $X_s(H_2)$ for H_2O_2-treated SConn-1 and NMx-2 are consistent with this expectation (see Figs. 2 and 3).

The proportions of trapped CO_2 in the total carbon of the samples of Figs. 2 and 3 were determined by extrapolation of these arrays to $X_s(H_2) = 0$. For untreated samples only the early portions of the arrays ($X_s(H_2) > 0.20$) were employed. These trapped CO_2 proportions and the measured concentrations of total carbon in the goethite were used to calculate the mineral-normalized concentrations of trapped CO_2 in the goethites. The trapped CO_2 concentrations for corresponding untreated and H_2O_2-treated goethite samples are listed in Table 1. Also listed in Table 1 are the concentrations of total carbon in corresponding untreated and H_2O_2-treated samples. The rather large differences between *total* carbon concentration before and after treatment with H_2O_2 are in sharp contrast to the generally unchanged values of *trapped* CO_2 concentrations before and after H_2O_2 treatment. The slightly higher calculated values for trapped CO_2 in untreated samples might reflect small contributions of CO_2 from organic matter. However, the good overall agreement between trapped CO_2 concentrations for corresponding untreated and H_2O_2-treated samples suggests that the peroxide treatment has had no measurable effect on the Fe(III) carbonate component in goethite.

The $\delta^{13}C$ values of CO_2 evolved from both untreated and H_2O_2-treated goethite samples are plotted in Figs. 3 and 4 against $X_v(CO_2)$. $\delta^{13}C_v$ is the $\delta^{13}C$ value of the cumulative sum of CO_2 evolved at a given value of $X_v(CO_2)$. The $\delta^{13}C_v$ values plotted in Figs. 3 and 4 were calculated from the incremental data in Tables 2 and 3 with the exception of untreated Paleo-X which was evolved in a manner that produced a directly measured $\delta^{13}C_v$ value for the single 230°C step of each of the four experiments (see Table 2). The $\delta^{13}C_v$ data for untreated NMx-2, SConn-1, and PPColo-1 were taken from

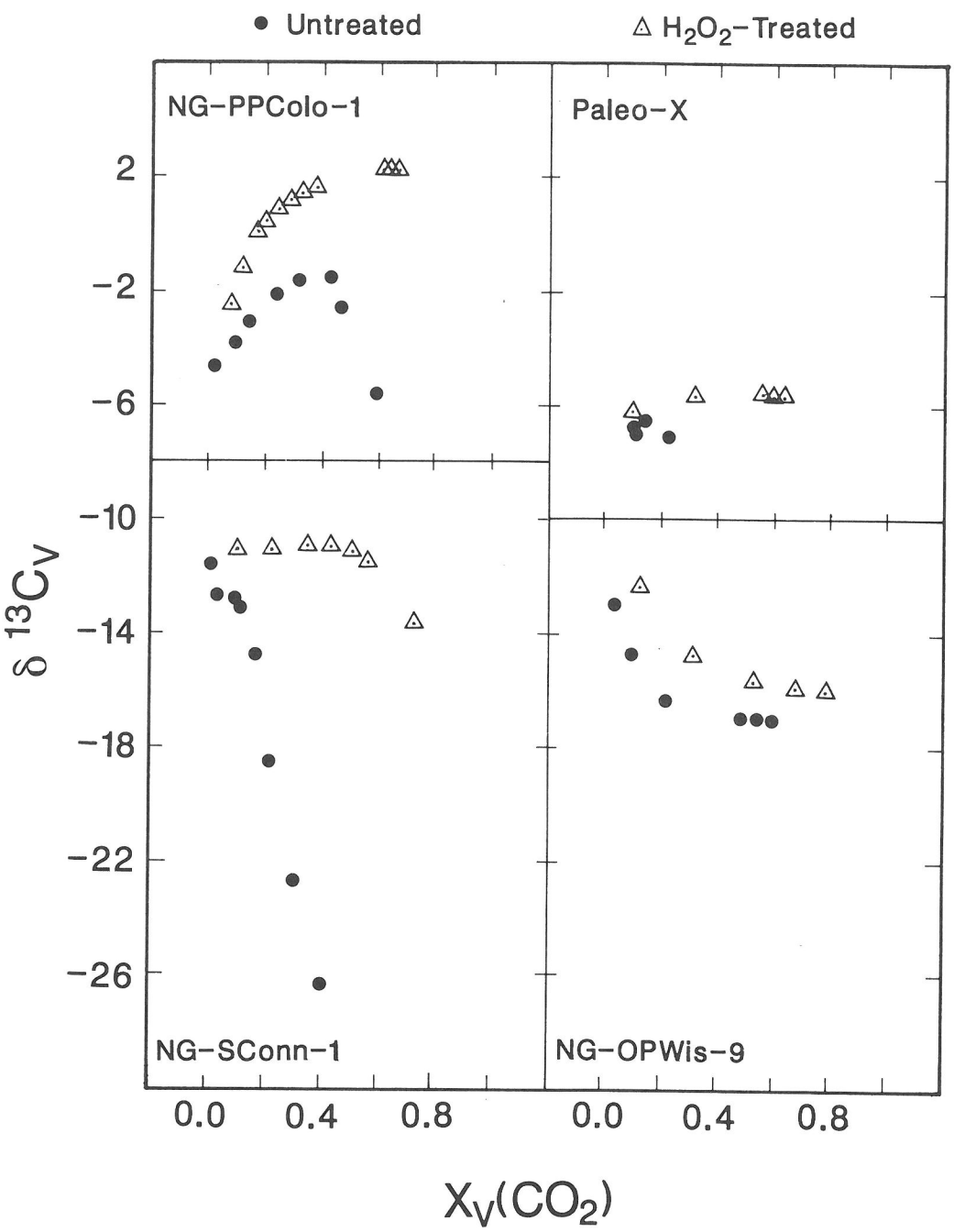

FIG. 4. $\delta^{13}C_v$ *vs.* $X_v(CO_2)$ for untreated and H_2O_2-treated aliquots of four different goethite samples. Note that the $\delta^{13}C_v$ values of the untreated aliquots are more negative than those of the corresponding H_2O_2-treated aliquots reflecting a contribution of ^{13}C-depleted CO_2 from organic matter in the untreated samples.

YAPP and POTHS (1986). The $\delta^{13}C_v$ parameter is employed here rather than the $\delta^{13}C$ values of non-cumulative, discrete increments of evolved CO_2, because the data of YAPP and POTHS (1986), which are used for comparison, were directly determined as $\delta^{13}C_v$. The plots in Figs. 3 and 4 reveal distinct isotopic differences between CO_2 evolved from untreated and H_2O_2-treated goethites. In all five cases

the $\delta^{13}C_v$ values of the H_2O_2-treated samples are more positive than those of the untreated samples. This isotopic distinction suggests that small amounts of organic-derived CO_2 contribute to the evolved CO_2 from untreated goethites even very early in the dehydration-decarbonation reaction. The two untreated samples with the largest concentrations of organic matter (NMx-2) and (SConn-1) exhibit the largest isotopic differences between evolved CO_2 from untreated and H_2O_2-treated samples as the reactions progress. The differences between treated and untreated $\delta^{13}C_v$ values can be as large as 17 per mil for NMx-2 (Fig. 3) and 14 per mil for SConn-1 (Fig. 4). These kinds of isotopic differences emphasize the importance of removal of organic matter before attempting to determine the carbon isotope composition of the Fe(III) carbonate (trapped CO_2) in goethites.

There are indications in the data for the H_2O_2-treated goethites of Figs. 3 and 4 that the $\delta^{13}C_v$ values may reach relatively constant or "plateau" values. However, $\delta^{13}C_v$ values representing later portions of the dehydration-decarbonation reactions contain isotopic "memories" of the earlier evolved CO_2, because the $\delta^{13}C_v$ value represents the $\delta^{13}C$ value of the cumulative sum of the CO_2 evolved to that point in an experiment. The $\delta^{13}C$ values of noncumulative, discrete increments of evolved CO_2 are preferable, because they provide the kind of information required for discussions of the model predictions represented by Eqns. (1) and (2) and Fig. 1. All of the data for H_2O_2-treated samples in Tables 2 and 3 are the noncumulative, incremental type. Subsequent discussions of both yield and isotope data employ these incremental results.

One test for linearity of the $X_s(CO_2)$ *vs.* $X_s(H_2)$ arrays of Figs. 2 and 3 is an examination of the value of the instantaneous slope of an array as a function of reaction progress measured by $X_v(CO_2)$. Values of the slopes of these arrays over finite increments were calculated as the ratios of $n(CO_2)$ to $n(H_2O)$. Values of $n(CO_2)$ and the corresponding $n(H_2O)$ are listed in Tables 2 and 3. Plots of incremental $n(CO_2)/n(H_2O)$ ratios *vs.* $X_v(CO_2)$ for the five different peroxide-treated samples are found in Figs. 5 and 6. The data for NMx-2 were plotted in Fig. 6 to minimize the clutter in Fig. 5. Samples OPWis-9 and Paleo-X exhibit relatively small variations in their $n(CO_2)/n(H_2O)$ ratios as the dehydration-decarbonation progresses (Fig. 5). The $n(CO_2)/n(H_2O)$ ratios for SConn-1 are also relatively constant for $X_v(CO_2)$ values up to about 0.50. Thus, given the analytical error associated with measurements of such small amounts of CO_2, the model prediction of a linear correlation between $X_s(CO_2)$ and $X_s(H_2)$ (*i.e.* constant slope) is largely realized by samples OPWis-9, Paleo-X, and SConn-1. The change in slope of the $X_s(CO_2)$ *vs.* $X_s(H_2)$ data for peroxide-treated SConn-1 that is indicated by the large increase in $n(CO_2)/n(H_2O)$ at $X_v(CO_2)$ values greater than 0.50 (Fig. 5) is reminiscent of the more abrupt change in slope noted for untreated SConn-1 (see Fig. 2). This suggests that not all of the organic matter was removed by the H_2O_2 treatment of SConn-1. Carbon isotope results to be discussed below are consistent with this suggestion.

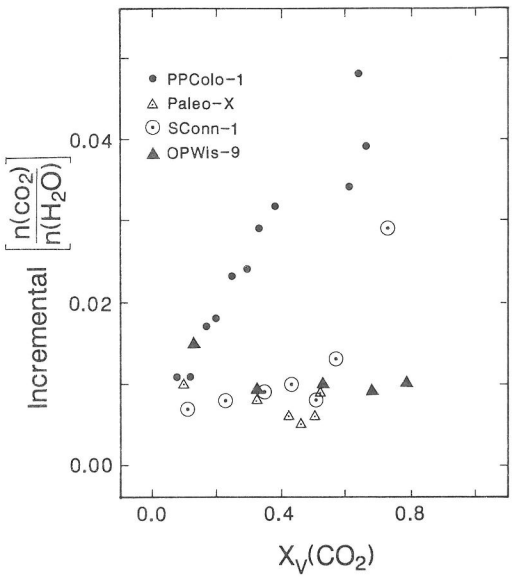

FIG. 5. A plot of the $n(CO_2)/n(H_2O)$ ratio for corresponding CO_2 and water increments evolved during vacuum dehydration-decarbonation of H_2O_2-treated goethite *vs.* $X_v(CO_2)$. Samples for which the loss of CO_2 is linearly correlated with loss of H_2O should yield horizontal data arrays in the diagram above. Three of the four samples exhibit intervals of very little change in the value of the $[n(CO_2)/n(H_2O)]$ ratio as a function of extent of reaction $[X_v(CO_2)]$. PPColo-1 has a continuously increasing ratio and SConn-1 exhibits an abrupt increase in the $n(CO_2)/n(H_2O)$ ratio at $X_v(CO_2)$ values greater than about 0.50 (see text for discussion).

As indicated by the $n(CO_2)/n(H_2O)$ *vs.* $X_v(CO_2)$ data of Figs. 5 and 6, the slopes of the $X_s(CO_2)$ *vs.* $X_s(H_2)$ arrays of peroxide-treated PPColo-1 and NMx-2 increase continuously as the dehydration-decarbonation reaction progresses. Consequently, the $X_s(CO_2)$ *vs.* $X_s(H_2)$ arrays are curvilinear for these samples. To determine if residual organic matter not removed by the H_2O_2 was contributing to the nonlinear behavior, a second aliquot of NMx-2 was subjected to vacuum dehydration-decarbonation (see experiment 1087 in Table 3). In this experiment the first step (after outgassing at 100°C)

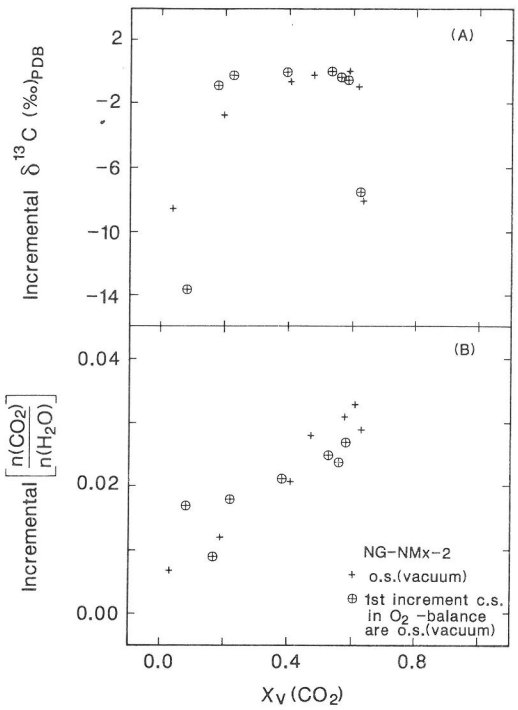

FIG. 6. The upper plot (A) shows the $\delta^{13}C$ values of increments of CO_2 evolved during dehydration-decarbonation of H_2O_2-treated NMx-2 *vs.* $X_v(CO_2)$. "O.S." refers to open-system vacuum dehydration conditions, while "C.S." refers to closed-system conditions. A "plateau" of $\delta^{13}C$ values near −0.2 per mil is evident in the $X_v(CO_2)$ range from about 0.10 to 0.50, particularly for the experiment for which the first CO_2 increment was recovered after closed-system dehydration in oxygen. Subsequent increments of CO_2 from this experiment were recovered during open-system dehydration in vacuum (see text for discussion). Plot (B) shows that the slope of the correlated loss of CO_2 and H_2O in H_2O_2-treated NMx-2 generally increases as the dehydration of the goethite progresses. The principal exception to this general trend is the first increment in the population represented by the circled crosses. This increment was obtained under closed-system conditions in O_2 (see Table 3) which facilitated oxidation of some of the small amounts of organic matter remaining after H_2O_2 treatment and thus increased its $n(CO_2)/n(H_2O)$ ratio.

involved a 200°C closed-system extraction in 0.16 bar of pure O_2 for one hour. As can be seen in Table 3, the amount of hydrogen extracted by the closed-system step was not much greater than that extracted by the first open-system step of experiment 1082. Yet, the $n(CO_2)/n(H_2O)$ ratio of the closed-system step in O_2 at 200°C (experiment MHD 1087) is larger than that in the first open-system step of experiment 1082 (see Fig. 6B). The larger value of the $n(CO_2)/n(H_2O)$ ratio for the oxidative closed-system step of MHD 1087 suggests that there was some organic matter remaining in this sample after H_2O_2 treatment. The $\delta^{13}C$ value of the CO_2 from the oxidative 200°C closed-system step of 1087 is more negative than that of the first open-system *in vacuo* step of 1082 (see Fig. 6A). The more negative $\delta^{13}C$ value of the closed-system CO_2 is consistent with the idea that the higher $n(CO_2)/n(H_2O)$ ratio of this step is a result of oxidation of a small amount of organic matter remaining in the sample. However, this residual organic matter is apparently not responsible for the nonlinear character of the $X_s(CO_2)$ *vs.* $X_s(H_2)$ data array of H_2O_2-treated NMx-2, because subsequent 200°C steps in experiment 1087 were run under open-system conditions in vacuum and the pattern of increasing $n(CO_2)/n(H_2O)$ ratios with increasing $X_v(CO_2)$ mimics that for experiment 1082 (see Fig. 6B). A similar experiment (unpublished) on a second aliquot of H_2O_2-treated PPColo-1 yielded the same type of pattern as that shown in Fig. 5 for PPColo-1. Therefore, it appears that the nonlinear $X_s(CO_2)$ *vs.* $X_s(H_2)$ arrays observed for peroxide-treated samples of PPColo-1 and NMx-2 are reproducible and are not related to the presence of small amounts of organic matter that were not removed by H_2O_2.

The assumptions adopted earlier for the model of Fe(III) carbonate in solid solution in goethite do not lead to a prediction of curvilinear behavior in $X_s(CO_2)$ *vs.* $X_s(H_2)$ plots. Although this curvilinear behavior seems to weaken support for the model, it is apparent from the carbon isotope data to be discussed later that the model of Fe(III) carbonate in goethite can explain all of the data obtained thus far, including those for the curvilinear $X_s(CO_2)$ *vs.* $X_s(H_2)$ arrays.

Figure 6A contains a plot of the $\delta^{13}C$ values of increments of evolved CO_2 *vs.* the cumulative progress variable $X_v(CO_2)$ for H_2O_2-treated NMx-2 (experiments 1082 and 1087). For both experiments the $\delta^{13}C$ values of the increments of evolved CO_2 are initially relatively negative then rapidly increase to a "plateau" of values near −0.2. In both experiments the final 200°C open-system vacuum dehydration steps were run for times in excess of 1000 minutes (see Table 3). The $\delta^{13}C$ of the CO_2 from this final long-term 200°C step was shifted to much more negative values in both experiments. Such negative $\delta^{13}C$ shifts in CO_2 evolved during a long-term vacuum dehydration step near the end of the reaction indicate that some of the evolved CO_2 originated from a small amount of organic matter which was only slowly oxidized to CO_2 (perhaps by reaction with the ferric oxide in the solid state at 200°C). With the small amounts of evolved CO_2 generated in these long duration final 200°C

steps (*ca.* 1 μmole, see Table 3), organically derived CO_2 could constitute 15 to 20% of the CO_2 sample and not have a measurable effect on the yield, because the analytical precision of the manometric measurements is only about ±0.15 μmole. Addition of as little as 0.2 to 0.3 μmole of organically derived CO_2 with a $\delta^{13}C$ value of *ca.* −35 (see YAPP and POTHS, 1986) to *ca.* 1 μmole of evolved trapped CO_2 with a $\delta^{13}C$ value of −0.2 would yield a composite evolved CO_2 sample with a $\delta^{13}C$ of less than −7.0. Note that the initial 200°C closed-system oxidation step of 1087 had no significant effect on the organic matter hypothesized to explain the isotopic shifts in the terminal 200°C steps. However, the $\delta^{13}C$ values of CO_2 evolved under vacuum at 200°C in steps subsequent to the initial oxidative closed-system step of 1087 almost immediately attained the "plateau" values near −0.2 (see Fig. 6A). This suggests that a small amount of easily oxidizable organic matter which interfered with the approach to plateau $\delta^{13}C$ values early in experiment 1082 was largely removed by the initial oxidative closed-system 200°C step of experiment 1087. The constancy of evolved CO_2 $\delta^{13}C$ values manifested in the isotopic plateau of Fig. 6A is consistent with the prediction of the Fe(III) carbonate model.

Samples of goethite which fulfill all of the stated predictions of the Fe(III) carbonate model would produce a characteristic data array on a plot of incrementally evolved trapped CO_2 $\delta^{13}C$ values *vs.* the corresponding $n(CO_2)/n(H_2O)$ ratios. If the trapped CO_2 $\delta^{13}C$ values and the $n(CO_2)/n(H_2O)$ ratios are each constant (as predicted) during the dehydration-decarbonation reaction of a goethite, all of the data for that goethite should be superposed on a single point in such a plot. The existence of analytical error suggests that a more realistic expectation would be for a relatively tight cluster of data points on such a diagram.

The $\delta^{13}C$ values of incrementally evolved CO_2 are plotted in Fig. 7 against the corresponding $n(CO_2)/n(H_2O)$ ratios for H_2O_2-treated samples PPColo-1, Paleo-X, SConn-1, and OPWis-9 (data are listed in Table 2). Paleo-X, SConn-1, and OPWis-9 all exhibit small domains of data points which reflect the relative constancy of the evolved CO_2 $\delta^{13}C$ values and the linearity of their $X_s(CO_2)$ *vs.* $X_s(H_2)$ slopes over most of the extent of goethite dehydration. The first CO_2 increment from OPWis-9 (experiment 1059, Table 2) has a higher $n(CO_2)/n(H_2O)$ ratio and a more positive $\delta^{13}C$ value than subsequent evolved CO_2 increments (Fig. 7). The tight cluster of the subsequent OPWis-9 data (Fig. 7) implies that the initial point in 1059 contains a CO_2 component that did not originate as trapped

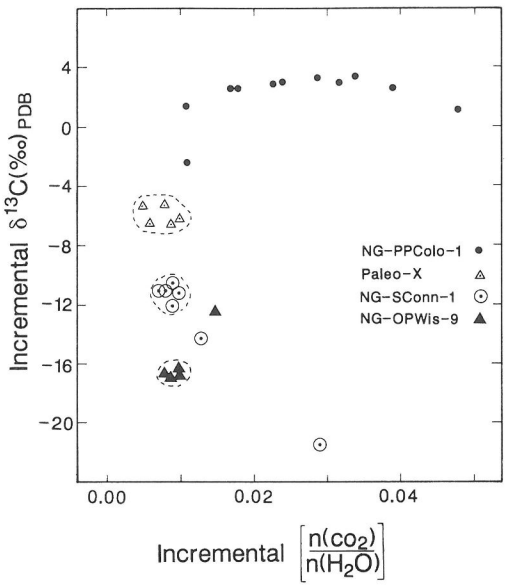

FIG. 7. Incremental $\delta^{13}C$ values *vs.* corresponding incremental $n(CO_2)/n(H_2O)$ ratios for H_2O_2-treated goethites. The model for Fe(III) carbonate in goethite that is discussed in the text predicts that in this type of plot all the data from a single goethite sample will plot on a common point. The enclosed data clusters in the diagram represent an approximate realization of the prediction. The data for PPColo-1 and three other apparently aberrant points are discussed in the text. All four of the samples in this figure exhibit "plateaus" of evolved CO_2 $\delta^{13}C$ values.

CO_2 in the goethite. This extra CO_2 in the initial 230°C step of OPWis-9 (1059) may contain a significant proportion of surface-adsorbed CO_2. Comparison of experiment 1059 with 1090 suggests that an initial closed-system oxidative step (1090) removes more of the extra "^{13}C-rich" CO_2, because subsequent trapped CO_2 $\delta^{13}C$ values in 1090 are more negative than in 1059. SConn-1 has five tightly grouped data points in Fig. 7 and two which display progressively larger $n(CO_2)/n(H_2O)$ ratios and more negative $\delta^{13}C$ values. The latter two points represent the two final 200°C *in vacuo* steps (see Table 2 and Fig. 5). In particular the SConn-1 data point with the largest $n(CO_2)/n(H_2O)$ ratio and the most negative $\delta^{13}C$ value represents the terminal 200°C *in vacuo* step which was run for 960 minutes. As was discussed earlier, the CO_2 from this step probably contains a portion of CO_2 that derived from the slow oxidation (by the ferric oxide?) of a small amount of organic matter which was not removed by the room temperature H_2O_2 treatment. The $\delta^{13}C$ value of −21.5 for the CO_2 evolved in this step is consistent with this suggestion. The enclosed domains of data for samples Paleo-X, SConn-1, and

OPWis-9 in Fig. 7 are assumed to represent the trapped CO_2(Fe(III) carbonate) in these samples, because these data represent a pattern of behavior predicted by the Fe(III) carbonate model.

The PPColo-1 data of Fig. 7 exhibit a "plateau" of $\delta^{13}C$ values which is close to +3 per mil. The initial 200°C step produced the CO_2 which is isotopically farthest removed from the plateau $\delta^{13}C$ values. The source for some of this initial CO_2 is unknown but may be surface-adsorbed CO_2 which was not outgassed at 100°C. The existence of relatively constant $\delta^{13}C$ values for the incrementally evolved CO_2 from both PPColo-1 (Fig. 7) and NMx-2 (Fig. 6A) is consistent with the origin of this CO_2 from a minor Fe(III) carbonate component in goethite in spite of the inconstancy of the $n(CO_2)/n(H_2O)$ ratio for each of these H_2O_2-treated samples. An Fe(III) carbonate origin for this CO_2 is supported by the infrared spectra of these same two samples (YAPP and POTHS, 1990).

We do not yet have an experimentally supported explanation for the nearly continuous increase of $n(CO_2)/n(H_2O)$ ratios during the course of dehydration-decarbonation experiments performed on H_2O_2-treated NMx-2 and PPColo-1. However, one speculation centers on the fact that these samples contain nonstoichiometric water which persists in the sample even after outgassing at 100°C (YAPP and PEDLEY, 1985). If this nonstoichiometric water were released at *ca.* 230°C in vacuum at a somewhat higher rate than the structural hydroxyl hydrogen (and trapped CO_2), the $n(CO_2)/n(H_2O)$ ratios early in the vacuum dehydration would be smaller. As the dehydration progressed this ratio would become progressively larger, because the proportion of nonstoichiometric water would diminish relative to structural water. Furthermore, the release of extraneous nonstoichiometric water should not affect the constancy of $\delta^{13}C$ values of CO_2 incrementally evolved from Fe(III) carbonate. Such behavior would explain the relatively constant trapped CO_2 $\delta^{13}C$ values over the range of $n(CO_2)/n(H_2O)$ values observed for NMx-2 and PPColo-1 (Figs. 6 and 7).

The preceding results and discussion indicate that the $\delta^{13}C$ values of the putative Fe(III) carbonate component in natural goethites can be measured and that the predictions of the Fe(III) carbonate model concerning goethite vacuum dehydration-decarbonation experiments are generally realized. The averaged "plateau" $\delta^{13}C$ values of the Fe(III) carbonates (trapped CO_2) in the five goethites of Tables 2 and 3 are as follows: OPWis-9 (−17.1); SConn-1 (−11.2); Paleo-X (−5.7); PPColo-1 (+2.9); NMx-2 (−0.2). This $\delta^{13}C$ range of about 20 per mil among these five samples suggests that information on the different environments of formation may be preserved in the Fe(III) carbonate in goethite.

Fe(III) carbonate $\delta^{13}C$ values and paleoenvironment

Figure 8 depicts the approximate $\delta^{13}C$ ranges of a number of low temperature carbon reservoirs. The 20 per mil range of $\delta^{13}C$ values measured for the Fe(III) carbonate component in the five natural goethites of the current study is comparable to the $\delta^{13}C$ range for "freshwater" carbonates. All five of the goethite samples of Table 1 have hydrogen and oxygen isotope ratios which indicate formation in the presence of meteoric ("fresh") waters (YAPP, 1987b; also, unpubl. results). Sedimentary calcite which had precipitated from an aqueous system in isotopic equilibrium with atmospheric CO_2 ($\delta^{13}C$ of −7) would be expected to have $\delta^{13}C$ values of about +3 or +4 (FRIEDMAN and O'NEIL, 1977). Because the $\delta^{13}C$ values of freshwater calcium carbonates of diverse origins appear to be controlled by the $\delta^{13}C$ values of the ambient aqueous carbonate + CO_2 system (FRITZ and POPLAWSKI, 1974; QUADE *et al.*, 1989), freshwater carbonates with $\delta^{13}C$ values significantly more negative then *ca.* +3 were probably precipitated from waters in which oxidized organic matter lowered the $\delta^{13}C$ value of the aqueous carbonate (Fig. 8). However, the possible role of other environmental parameters in controlling carbonate $\delta^{13}C$ values needs to be evaluated to determine how directly the different $\delta^{13}C$ values of solid carbonates reflect differences in the $\delta^{13}C$ values of the ambient aqueous carbonate systems.

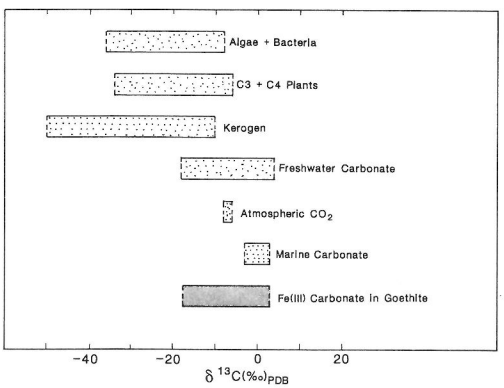

FIG. 8. Approximate ranges of $\delta^{13}C$ values for a number of surficial carbon reservoirs. Ranges were taken from HOEFS (1987) and SCHIDLOWSKI *et al.* (1983). The range of $\delta^{13}C$ values exhibited by the putative Fe(III) carbonate (trapped CO_2) in the goethite samples of the current study is shown for comparison.

The carbon isotope fractionation factor for Fe(III) carbonate *vs.* CO_2 is not yet known. However, CAROTHERS *et al.* (1988) experimentally determined the α for $^{13}C/^{12}C$ partitioning between siderite and CO_2. Comparison of the siderite-CO_2 fractionation at the lowest experimental temperature (33°C) reported by CAROTHERS *et al.* (1988) with the calcite-CO_2 fractionation at 33°C (FRIEDMAN and O'NEIL, 1977) reveals that siderite would be enriched in ^{13}C by about 2.6 per mil relative to calcite. Over the range of sedimentary and early diagenetic temperatures (<100°C) it appears as if the carbon isotope fractionation between siderite and calcite does not vary greatly with temperature. By analogy it will be assumed as a first approximation that the carbon isotope fractionation between Fe(III) carbonate and calcite is independent of temperature and that the temperature dependence which applies to the calcite-CO_2 α also applies, with a constant correction, to $^{13}\alpha$ for Fe(III) carbonate *vs.* CO_2.

OHMOTO (1972) pointed out the influence of pH on the $\delta^{13}C$ values of different aqueous carbonate species in hydrothermal systems. pH in low temperature carbonate systems is not often considered as a variable of isotopic importance, because sedimentary calcite precipitation commonly occurs in systems with pH values of about 7 to 8.5 (*e.g.*, WHITE *et al.*, 1963; HOLLAND, 1978). CRERAR *et al.* (1979) have studied the bog iron of the New Jersey pine barrens. The ferric hydroxides (including goethite) which make up these deposits seem to have been precipitated from water with pH values ranging from about 4.1 to 5.7. Tropical lateritic soils in which goethite is abundant commonly have pH values around 4 or 5 (SOIL SURVEY STAFF, 1975). In addition, goethites which are pseudomorphs after pyrite or siderite can be expected to have formed in low pH environments because of the formation of sulfuric acid and carbonic acid, respectively, during goethite formation. Thus, the carbon isotope fractionation between the minor Fe(III) carbonate component in goethite and the total aqueous carbonate system may originate in relatively low pH environments. Inspection of the temperature dependence of the carbon isotope fractionation factors for calcite-CO_2 and aqueous carbonate-CO_2 (FRIEDMAN and O'NEIL, 1977) suggests, by analogy, that the extent to which variations in temperature will cause variations in Fe(III) carbonate $\delta^{13}C$ values should be related to the pH of the environment.

The following closed-system equation represents the equilibrium carbon isotope fractionation (ϕ) between calcite and total aqueous carbonate as a function of hydrogen ion activity and temperature. The temperature dependence of ϕ arises through the temperature dependence of α(a-b), α(cc-b), K_1 and K_2:

$$\phi = \frac{R_{cc}}{R_{tot}} = \frac{\alpha(\text{cc-b})}{A + B + C} \tag{3}$$

where

$$A = \frac{\alpha(\text{a-b})}{1 + \frac{K_1}{a_H} + \frac{K_1 K_2}{a_H^2}}$$

$$B = \frac{1}{\frac{a_H}{K_1} + 1 + \frac{K_2}{a_H}}$$

$$C = \frac{\alpha(\text{c-b})}{\frac{a_H^2}{K_1 K_2} + \frac{a_H}{K_2} + 1}$$

R_{cc} = $^{13}C/^{12}C$ of calcite

R_{tot} = $^{13}C/^{12}C$ of total dissolved carbonate ($CO_2 + HCO_3^- + CO_3^=$)

α(cc-b) = α for carbon isotope fractionation between calcite and dissolved bicarbonate

α(c-b) = $^{13}\alpha$ for dissolved carbonate *vs.* bicarbonate

α(a-b) = $^{13}\alpha$ for neutral aqueous CO_2 *vs.* bicarbonate

a_H = hydrogen ion activity

K_1 = first acid dissociation constant of H_2CO_3

K_2 = second acid dissociation constant of H_2CO_3

Dilute solution conditions were assumed. It was also assumed that α(c-b) did not vary with temperature. Over the temperature range employed in these calculations, the latter assumption appears to be reasonable (FRIEDMAN and O'NEIL, 1977). The temperature dependence of K_1 and K_2 was determined from tabulations in DREVER (1982). The temperature dependence of α(cc-b) and α(a-b) was determined from graphs in FRIEDMAN and O'NEIL (1977).

A plot of 1000 ln ϕ *vs.* T (°C) at two different pH values is given in Fig. 9. As can be seen in Fig. 9, the temperature dependence of ϕ is greater at pH 4 than at pH 8. Furthermore, at a particular temperature, ϕ is larger at pH 4 than at 8. The temperature of formation for the goethites of Table 1 might range from about 10 to 30°C as determined with hydrogen and oxygen isotopes (YAPP, 1987b and unpubl. results). At pH 4 and treating variations of ϕ as a proxy for variations of Fe(III) carbonate,

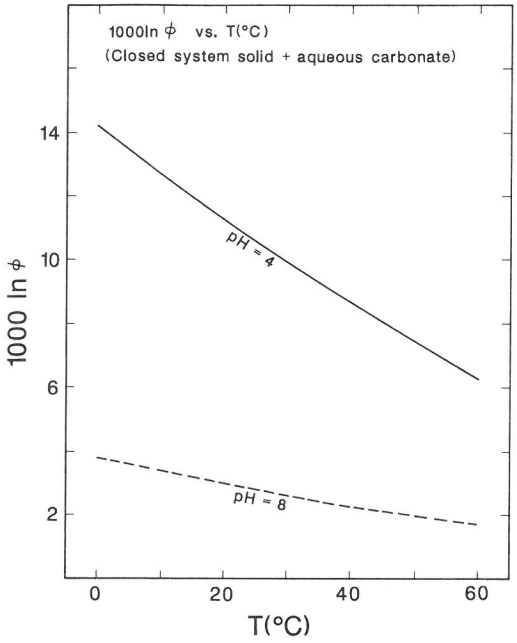

FIG. 9. 1000 ln ϕ *vs.* T (°C) calculated at pH values of 4 and 8. ϕ is the equilibrium ratio of $^{13}C/^{12}C$ in calcite to $^{13}C/^{12}C$ in total aqueous carbonate under closed-system conditions. Note that the temperature dependence of ϕ is greater at low pH than at high pH.

Fig. 9 suggests that a temperature-controlled $\delta^{13}C$ range of about 2.7 per mil could result if the aqueous total carbonate $\delta^{13}C$ value were constant. Therefore, only about 14% of the observed 20 per mil range of goethite trapped CO_2 $\delta^{13}C$ values might be explained by differences in temperatures of formation.

As a further illustration of the effect of pH, it is assumed that Fe(III) carbonate carbon isotope systematics are the same as those of siderite. Figure 10 contains curves which depict the closed-system variation of Fe(III) carbonate (trapped CO_2) $\delta^{13}C$ values as a function of pH at 30°C. Curve A assumes that the total aqueous carbonate has a $\delta^{13}C$ value of −24 per mil, while curve B assumes a $\delta^{13}C$ value of −29 per mil. As can be seen in Fig. 10, the Fe(III) carbonate $\delta^{13}C$ values are insensitive to variations in pH at values less than about 5 and greater than about 7.5. Although shifts in pH over the range from 5 to 7.5 could produce about a six per mil shift in the goethite trapped CO_2 $\delta^{13}C$ value at 30°C in a closed system, pH-induced shifts of this magnitude are too small to explain the 20 per mil range observed in the Fe(III) carbonates of diverse goethites. Thus, although temperature and pH need to be considered, much of the Fe(III) carbonate $\delta^{13}C$ range of the goethites of Table 1 is probably a consequence of the original environmental CO_2 $\delta^{13}C$ values.

CONCLUSIONS

The dominant component in the small amounts of carbon dioxide evolved from H_2O_2-treated natural goethites during dehydration experiments in vacuum at *ca.* 230°C appears to be "trapped" CO_2 from a minor Fe(III) carbonate component apparently in solid solution in the goethites. Patterns of coupled CO_2-H_2O release and incremental CO_2 $\delta^{13}C$ values are largely those expected for the hypothesized Fe(III) carbonate. The $\delta^{13}C$ range of about 20 per mil observed for trapped CO_2 from the different samples analyzed in this study indicates that information about the respective environments of formation is preserved in the carbon isotope ratios of Fe(III) carbonate in goethite. Temperature and pH may affect the $\delta^{13}C$ value of Fe(III) carbonate, but much of the observed $\delta^{13}C$ range of 20 per mil among diverse goethites is probably due to differences in the $\delta^{13}C$ values of ambient aqueous carbonate in the various environments of goethite for-

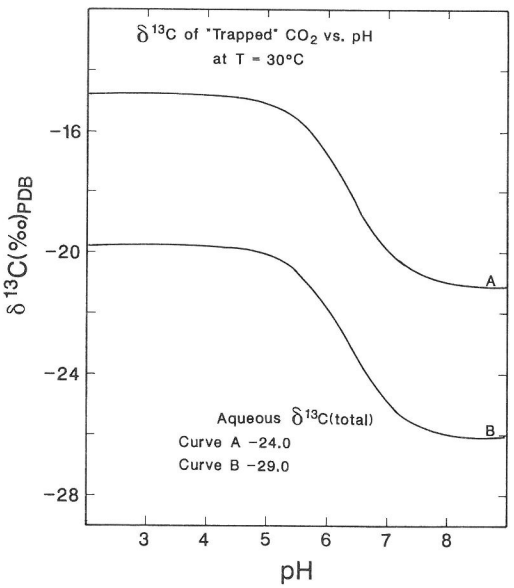

FIG. 10. $\delta^{13}C$ of Fe(III) carbonate (trapped CO_2) in goethite as a function of pH at 30°C for two different total aqueous carbonate $\delta^{13}C$ values. Closed-system conditions and Fe(III) carbonate ≪ total aqueous carbonate were two of the assumptions employed to calculate these curves. At this temperature pH changes alone are capable of producing a trapped CO_2 $\delta^{13}C$ range of about six per mil. However, most of this pH dependency occurs in the pH range from about 5.0 to 7.5. Above and below these pH values, the $\delta^{13}C$ value is insensitive to pH changes.

mation. Consequently, goethite-trapped CO_2 $\delta^{13}C$ values represent a new indicator of variation in ancient near-surface environmental conditions.

Acknowledgements—It is difficult to properly acknowledge someone who was such an outstanding mentor, but one of your former graduate students says, "Thanks, Sam." Dag Lopez drafted the figures, and this manuscript was typed by Marie Tenorio, Mary Sherman, and Mabel T. Chavez. This research was supported by NSF grants EAR-8719070 and EAR-9003108.

REFERENCES

CAROTHERS W. W., ADAMI L. H. and ROSENBAUER R. J. (1988) Experimental oxygen isotope fractionation between siderite-water and phosphoric acid liberated CO_2-siderite. *Geochim. Cosmochim. Acta* **52,** 2445–2450.

CRAIG H. (1957) Isotopic standards for carbon and oxygen and correction factors for mass-spectrometric analysis of carbon dioxide. *Geochim. Cosmochim. Acta* **12,** 133–149.

CRERAR D. A., KNOX G. W. and MEANS J. L. (1979) Biogeochemistry of bog iron in the New Jersey pine barrens. *Chem. Geol.* **24,** 111–135.

DREVER J. I. (1982) *The Geochemistry of Natural Waters.* Prentice-Hall.

DVORAK V., FEITKNECHT W. and GEORGES P. (1969) Sur les carbonates basiques de fer (III): I. Carbonate basique de fer (III) amorphe. *Helv. Chim. Acta* **52,** 501–515.

FRIEDMAN I. and O'NEIL J. R. (1977) Compilation of stable isotope fractionation factors of geochemical interest. *U.S. Geol. Surv. Prof. Pap.* 440-K; *Data of Geochemistry,* 6th ed.

FRITZ P. and POPLAWSKI S. (1974) ^{18}O and ^{13}C in the shells of freshwater molluscs and their environments. *Earth Planet. Sci. Lett.* **24,** 91–98.

HOEFS J. (1987) *Stable Isotope Geochemistry,* 3rd ed. Springer-Verlag, Berlin.

HOLLAND H. D. (1978) *The Chemistry of the Atmosphere and Oceans.* J. Wiley & Sons.

OHMOTO H. (1972) Systematics of sulfur and carbon isotopes in hydrothermal ore deposits. *Econ. Geol.* **67,** 551–578.

PAULL R. A. (1977) The Upper Ordovician Neda Formation of Eastern Wisconsin. In *Geology of Southern Wisconsin* (ed. K. G. NELSON); *A Guidebook for the 41st Annual Tri-State Field Conference, Wisconsin Geol. Nat. Hist. Surv.,* pp. C-1 to C-18.

QUADE J., CERLING T. E. and BOWMAN J. R. (1989) Systematic variations in the carbon and oxygen isotopic composition of pedogenic carbonate along elevation transects in the southern Great Basin, United States. *Geol. Soc. Amer. Bull.* **101,** 464–475.

SCHIDLOWSKI M., HAYES J. M. and KAPLAN I. R. (1983) Isotopic inferences of ancient biochemistries: Carbon, sulfur, hydrogen and nitrogen. *In Earth's Earliest Biosphere Its Origin and Evolution* (ed. J. W. SCHOPF), pp. 149–186. Princeton University Press.

SOIL SURVEY STAFF (1975) *Soil Taxonomy.* U.S. Dept. of Agriculture and U.S. Government Printing Office, *Agriculture Handbook 436,* Washington, D.C.

WHITE D. E., HEM J. D. and WARING G. A. (1963) Chemical composition of subsurface waters, In *Data of Geochemistry; U.S. Geol. Surv. Prof. Pap. 440-f,* 6th ed.

YAPP C. J. (1983) Stable hydrogen isotopes in iron oxides-isotope effects associated with the dehydration of a natural goethite. *Geochim. Cosmochim. Acta* **47,** 1277–1287.

YAPP C. J. (1987a) A possible goethite-iron (III) carbonate solid solution and the determination of CO_2 partial pressures in low temperature geologic system. *Chem. Geol.* **64,** 259–268.

YAPP C. J. (1987b) Oxygen and hydrogen isotope variations among goethites (α-FeOOH) and the determination of paleotemperatures. *Geochim. Cosmochim. Acta* **51,** 355–364.

YAPP C. J. and PEDLEY M. D. (1985) Stable hydrogen isotopes in iron oxides—II. D/H variations among natural goethites. *Geochim. Cosmochim. Acta* **49,** 487–495.

YAPP C. J. and POTHS H. (1986) Carbon in natural goethites. *Geochim. Cosmochim. Acta* **50,** 1213–1220.

YAPP C. J. and POTHS H. (1990) Infrared spectral evidence for a minor Fe(III) carbonate-bearing component in natural goethite. *Clays Clay Mineral.* **38,** 442–444.